PHYSICAL REVIEW C **83**, 042801(R) (2011)

Direct measurement of the ^{18}F(p,α)^{15}O reaction at nova temperatures

C. E. Beer,[1] A. M. Laird,[1,*] A. St. J. Murphy,[2] M. A. Bentley,[1] L. Buchman,[3] B. Davids,[3] T. Davinson,[2] C. A. Diget,[1] S. P. Fox,[1] B. R. Fulton,[1] U. Hager,[3,†] D. Howell,[3] L. Martin,[3] C. Ruiz,[3] G. Ruprecht,[3] P. Salter,[2] C. Vockenhuber,[3,‡] and P. Walden[3]

[1]*Department of Physics, University of York, York YO10 5DD, United Kingdom*

[2]*SUPA, School of Physics and Astronomy, The University of Edinburgh, Edinburgh EH9 3JZ, United Kingdom*

[3]*TRIUMF, Vancouver, British Columbia V6T 2A3, Canada*

(Received 16 December 2010; published 12 April 2011)

The ^{18}F$(p,\alpha)^{15}$O reaction rate is crucial for understanding the final abundance of ^{18}F predicted by nova models. The γ-ray emission in the first few hours after a nova outburst is expected to be dominated by 511 keV annihilation photons from the decay of ^{18}F, and so understanding its production can provide important constraints on the conditions during the outburst when compared with observations. Results are presented from the lowest-energy direct measurement to date, performed at the Isotope Separator and Accelerator radioactive beam facility at the TRIUMF laboratory, Canada. Cross section measurements at center-of-mass energies of 250, 330, 453, and 673 keV are obtained and the results compared to previous data and R-matrix calculations. The implications for the overall reaction rate in the context of nova explosions have been discussed.

DOI: 10.1103/PhysRevC.83.042801 PACS number(s): 26.30.Ca, 24.30.−v, 25.40.Hs, 29.38.Gj

Novae are the third most energetic stellar explosions in the universe, after gamma-ray bursts and supernovae. These outbursts occur in binary systems consisting of a white dwarf and a less evolved companion star. Accretion of hydrogen-rich material from the outer envelope of the companion star onto the surface of the white dwarf leads to thermonuclear runaway (TNR) driven by the CNO cycle [1]. At higher temperatures, the nuclear processing and energy generation proceed via the hot-CNO cycles. In the first few hours, before the optical light curve is observed, γ-ray emission is thought to be dominated by annihilation photons from the β decay of ^{18}F. Direct observations of this γ-ray emission could provide a unique probe of the conditions (temperature, density, and timescales) during the TNR if the uncertainties in the relevant nuclear reaction rates are sufficiently constrained.

Within the hot-CNO cycle, ^{18}F is produced via ^{17}O$(p,\gamma)^{18}$F and by the β decay of ^{18}Ne. These production mechanisms are sufficiently well constrained that the main uncertainty in the final abundance of ^{18}F in novae arises from the destruction reactions, ^{18}F$(p,\alpha)^{15}$O and ^{18}F$(p,\gamma)^{19}$Ne. At the relevant temperatures, the former reaction is expected to dominate by roughly a factor of 1000 [2] and it is the uncertainty in this reaction rate which is the main nuclear contribution to the overall uncertainty in the ^{18}F abundance.

The ^{18}F$(p,\alpha)^{15}$O reaction has been the focus of considerable experimental effort in the last two decades (see Ref. [3] and references therein). Indirect techniques have been exploited to determine the parameters of key levels in ^{19}Ne and direct measurements were made down to energies just inside the Gamow window for ONe novae [4]. Despite significant progress, the reaction rate in the energy region covering nova temperatures is still unknown by at least an order of magnitude [5]. This uncertainty arises from the following unknowns: the role of the 8- and 38 keV resonances and their possible interference with the 665 keV $3/2^+$ resonance; the existence and contribution of the predicted $1/2^+$ resonances at -0.4 and 1.5 MeV [6–8]; and the contribution of a subthreshold state at -121 keV and its possible interference with above-threshold resonances [9].

To constrain the cross section, and thus the contribution from different interference terms, at low energies, a direct measurement of the ^{18}F$(p,\alpha)^{15}$O reaction was undertaken at effective center-of-mass energies of 250, 330, 453, and 673 keV. The 665 keV resonance has been well studied (see Refs. [10,11] and references therein), and so a measurement in this region allowed the validity of the technique to be confirmed. The 453 keV energy was chosen because it falls between two previous measurements by de Séréville *et al.* [12], at 402 and 486 keV, and would allow the presence of a possible $3/2^-$ resonance at 430(30) keV to be determined. The third energy measurement allowed an independent measurement of the 330 keV resonance, previously studied directly by Bardayan *et al.* [4]. However, the main aim of the present work was to measure the cross section below the 330 keV resonance to constrain the contribution from interference, between the $3/2^+$ states, in the Gamow window for nova events. We report here a direct measurement of the ^{18}F$(p,\alpha)^{15}$O cross section at 250 keV, the lowest energy to date.

The measurement was performed at the Isotope Separator and Accelerator (ISAC) radioactive beam facility, TRIUMF, Canada, utilizing a high-intensity (average 5×10^6 pps) ^{18}F^{4+} beam. The ^{18}O contamination in the beam, which was monitored throughout the experiment, dropped from an initial 70% (during 673 keV runs) to less than 5% during the 250 keV data runs. The ^{18}F beam was focused onto a $(CH_2)_n$ target located within the TRIUMF UK Detector Array (TUDA) scattering chamber. The beam intensity was monitored in real time with a Faraday cup and the beam constituents were determined by using monitor detectors positioned downstream of the

*Corresponding author: alison.laird@york.ac.uk

†Present address: Colorado School of Mines, Golden, Co, USA.

‡Present address: ETH Zurich, Zurich, Switzerland.

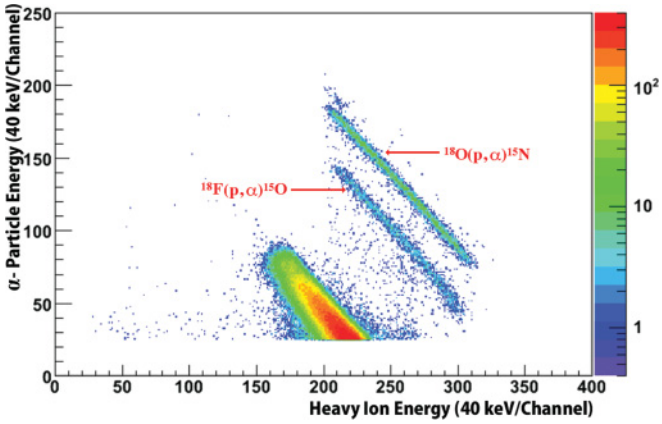

FIG. 1. (Color online) Energy in LEDA-1 vs energy in S2-2. The ^{18}F$(p,\alpha)^{15}$O (lower) and ^{18}O(p,α)^{15}N (upper) loci are highlighted, clearly separated from the broad elastic scattering feature. No cuts have been applied, apart from a 1 MeV threshold on all energies.

target at $\theta_{\rm lab} \sim 3^\circ$. A monolithic silicon detector [13] provided $\Delta E/E$ information to separate ^{18}O and ^{18}F. These data were complemented by direct beam data, using an attenuated beam between runs, from a Hamamatsu photodiode, located behind a 2-μm aluminum foil and mounted on the target ladder. This foil provided sufficient differential stopping such that ^{18}F and ^{18}O could be distinguished. The hydrogen content of the target was monitored by measuring the ratio of hydrogen to carbon recoils scattered, at a given angle, by the beam. When the ratio dropped significantly, the target was replaced. Two targets were used during the experiment, with thicknesses of 32 ± 2 and 34 ± 2 μg/cm^2, respectively.

Coincident α-particle and heavy-ion products were detected by highly segmented silicon strip detector arrays, providing particle energy, time-of-flight, and scattering angle information. One MSL YY1 LEDA (LEDA-2) [14] silicon strip detector was positioned upstream covering $\theta_{\rm lab} = 120^\circ$–$146^\circ$ and three further silicon strip detector arrays, one LEDA (LEDA-1) and two S2s (S2-1 and S2-2) [15], covered downstream laboratory angles of 4°–69°. Energy calibration of the silicon detectors was accomplished by using a standard ^{238}Pu-^{241}Am-^{243}Cm α-source. Figure 1 shows the raw energy-energy spectrum for coincident events at $E_{\rm c.m.} = 673$ keV ($E_{\rm beam} = 12.96$ MeV). The kinematic loci of ^{18}F$(p,\alpha)^{15}$O ($Q = 2.882$ MeV) and ^{18}O$(p,\alpha)^{15}$N events ($Q = 3.981$ MeV) can be clearly seen, and are well separated, above the broad feature due to elastically scattered ^{18}F and ^{18}O.

The presence of the ^{18}O contamination allowed normalization of the measured ^{18}F$(p,\alpha)^{15}$O yield to the known ^{18}O$(p,\alpha)^{15}$N cross sections (average of Refs. [16] and [17]) at the two highest energies. At the lower two energies, there were insufficient ^{18}O$(p,\alpha)^{15}$N events to allow this technique to be used and here the yield was normalized by comparison to Rutherford scattering from the ^{12}C in the target. The consistency of the two techniques was confirmed by using the 673 keV data.

Coincidence events of interest were then identified by selecting on summed energy, coplanarity, and opening angle, the latter of which was particularly effective. Figure 2 shows,

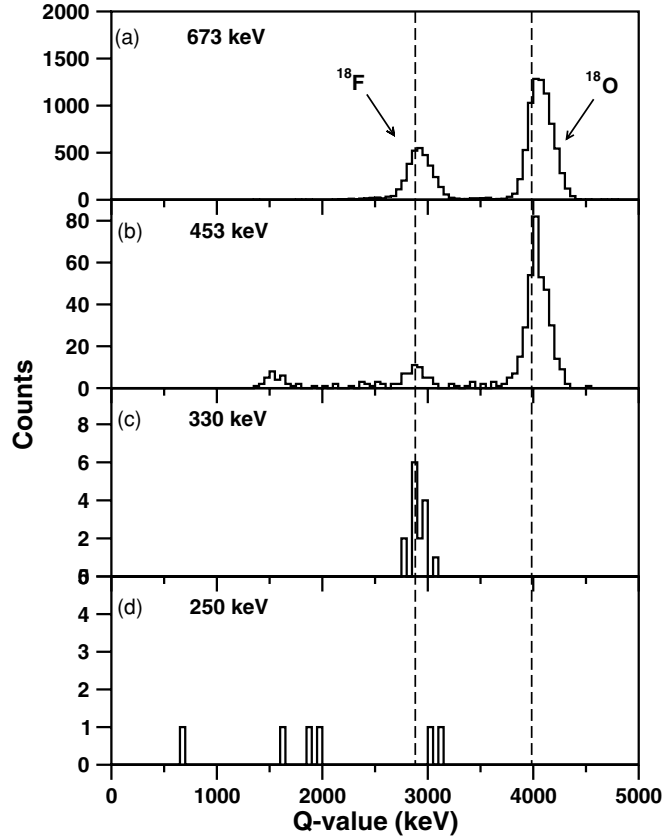

FIG. 2. Reaction Q values calculated from α-particle energy (uncorrected for energy loss in the target and detector dead layer) and angle, for all four energies, for coincident events in LEDA-1 vs S2-2. Gates applied to each energy are coplanarity, sum energy, and $\theta_{\rm LEDA\text{-}1}$ versus $\theta_{\rm S2\text{-}2}$.The vertical dotted lines indicate the ^{18}F$(p,\alpha)^{15}$O and ^{18}O$(p,\alpha)^{15}$N Q values.

for these events, the Q value (uncorrected for energy loss), at each beam energy, calculated from the α particle's energy and angle, assuming the reaction to be ^{18}F$(p,\alpha)^{15}$O. At $E_{\rm c.m.} = 250$ keV, there are two events of interest that are well separated from elastic scattering events at lower Q values.

For all energies except 330 keV (which is assumed to be an $\ell = 1$ transfer), the angular distributions were assumed to be isotropic, and the total reaction cross sections were obtained by multiplying the differential cross sections by 4π. For the 330 keV data, the measured angular distribution was fitted with an $\ell = 1$ Legendre polynomial and the integral over this polynomial was calculated to give the total cross section. The total cross sections for the present data are given in Table I and the calculated astrophysical S factors are shown in Fig. 3 with previous data sets for comparison. Error bars include statistical and systematic contributions. The uncertainty for the data point at 250 keV is entirely dominated by the low statistics and was calculated according to the Feldman-Cousins approach [18], based on two events with no background. The error bars indicate 68%, 90%, and 95% confidence levels. The assumption of zero background in the region of interest (2500–3500 keV in Fig. 2) was validated by using a time-of-flight gate on the data. The events at lower Q values

TABLE I. ^{18}F$(p,\alpha)^{15}$O cross sections and S factors.

$E_{\text{c.m.}}$ (keV)	σ (mb)	S factor (MeV barn)
673	$(0.47 \pm 0.14) \times 10^3$	$(1.3 \pm 0.4) \times 10^4$
453	1.1 ± 0.4	$(2.0 \pm 0.8) \times 10^2$
330	0.6 ± 0.3	$(8 \pm 4) \times 10^2$
250	$(12^{+14}_{-8}) \times 10^{-3}$	(110^{+120}_{-70})

(below 2000 keV) had time-of-flight values consistent with carbon recoils from elastic scattering. The cross section data point from the present work at 673 keV agrees well with existing data. The point at 453 keV neither indicates nor excludes the presence of the possible resonance at 430 keV, and further measurements with improved statistics are needed. The 330 keV data point agrees with the work of Bardayan *et al.* [4] within errors.

Multichannel R-matrix calculations were performed using the DREAM code [20] to calculate the astrophysical S factor from the 10 above-threshold resonances given in Table II. The level information used is taken from Ref. [3] with the addition of a $3/2^+$ state at 1347 keV observed by Murphy *et al.* [7]. The R-matrix channel radius parameter used was 5 fm, and an energy resolution of 15 keV (full width at half maximum) was assumed.

Interference between resonances of the same spin-parity results in significant differences in the S factor in the inter-resonance regions. For the five $3/2^+$ resonances included, 16 phases are possible. Within the energy region of interest, interference between the 8-, 38-, and 665 keV resonances

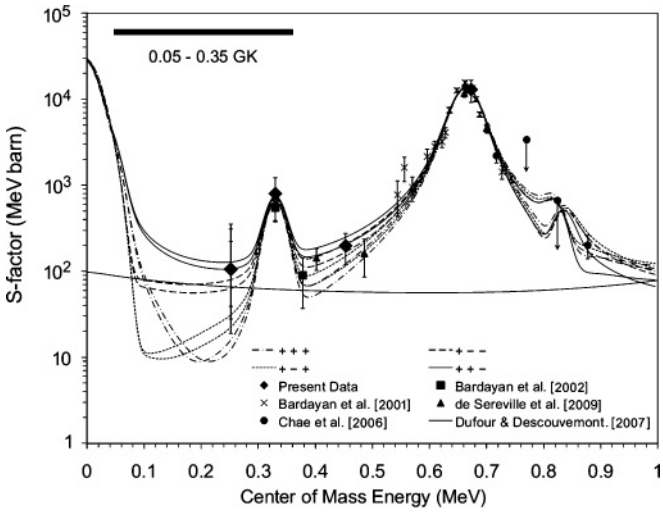

FIG. 3. The ^{18}F$(p,\alpha)^{15}$O S factors, calculated using the R matrix, for eight possible interference terms. The range in possible S factors arises from the interference between the $J^\pi = 3/2^+$ resonances. The interference between resonances dominates in the region of interest, resulting in four groups of S-factor curves. The upper and lower curves of each group are shown in the figure. The legend gives the assumed phase, for the 8-, 38-, and 665 keV resonances, respectively, for each pair of curves. Also plotted are the measured S factors from this work, those from previously published data [4,10,12,19], and the proposed contribution from $1/2^+$ states predicted in Ref. [6].

TABLE II. Resonance parameters used for the R-matrix calculations of the ^{18}F$(p,\alpha)^{15}$N S factor. Except where indicated, parameters are taken from Ref. [3].

E_{res} (keV)	J^π	Γ_p (keV)	Γ_α (keV)
-121	$1/2^+$	306[a]	11.6
8	$(3/2^-)$	7.19×10^{-39}	0.5
26	$1/2^-$	1.1×10^{-20}	220
38	$(3/2^+)$	4×10^{-15}	1.3
287	$(5/2^+)$	1.2×10^{-5}	1.2
330	$3/2^-$	2.22×10^{-3}	5.2
665	$3/2^+$	15.2	23.8
827	$3/2^+$	0.35	6
842	$(1/2^+)$	0.2	23
1089	$5/2^+$	1.25	0.24
1347[b]	$3/2^+$	42	5

[a]Reduced proton width taken from Ref. [9].
[b]Parameter taken from Ref. [7].

causes the greatest variation. This results in four groupings of S factors, with the width of each group reflecting the effects of the interference between the remaining two resonances (827 and 1347 keV). The upper and lower S factor curves for each group are shown in Fig. 3. As can be seen, the lowest-lying group of S-factor curves is strongly disfavored (>95%) by the data point at 250 keV, whereas the second-lowest group is weakly disfavored.

Neither of the two $1/2^+$ resonances (-0.41 and 1.49 MeV) predicted by Dufour and Descouvemont [6] are included in the present R-matrix calculations but their predicted contribution is shown in Fig. 3 for comparison. The interference between the two states is negligible [6] and their contribution may be approximated by the sum of these two isolated states. The 1.49 MeV resonance was observed via inelastic scattering of ^{19}Ne by Dalouzy *et al.* [8] but was not seen in elastic scattering by Murphy *et al.* [7]. The 1.49 MeV state, if it is present, does not make a significant contribution at nova temperatures, contrary to the conclusions of Dalouzy *et al.* [8], but its observation (or lack thereof) would indicate the existence (or not) of the -0.41 MeV resonance which, due to the predicted width of around 230 keV, does make a significant contribution in the relevant region. Further experiments to clarify the existence of both states are therefore important. There is a known state in ^{19}Ne at 6.013 MeV ($E_R = -0.398$ MeV), but this state is considered to be either $3/2^-$ or $1/2^-$ [21] and is not broad enough [22] to be the predicted -0.41 MeV resonance.

The picture is further complicated by recent indications that the 8 keV resonance may be a $3/2^-$ and that there is a significant contribution from a subthreshold $\ell = 0$ state at -121 keV [9]. However, recent data obtained by Josephides *et al.* [23], using ^{15}O(α,α) scattering, suggests that a state in this energy region, which may be the same state, is most consistent with a $5/2^+$ assignment. The recent compilation by Iliadis *et al.* [5] assumed the -121 keV state to be $1/2^+$ and the 8 keV state to be $3/2^-$.

The S factor calculated with these assumptions (all other parameters held as before and not including the 1089- and 1347 keV resonances, as per Ref. [5]) is shown in Fig. 4. The

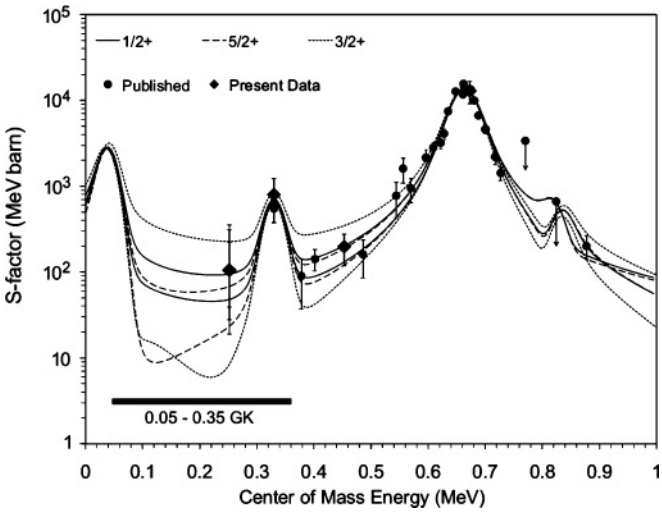

FIG. 4. Calculated ^{18}F$(p,\alpha)^{15}$O S factors with the 8 keV state treated as having a spin-parity of $3/2^-$ using the Adekola parameters [9]. The six curves correspond to the upper and lower S factors, assuming the -121 keV resonance to be $1/2^+$, $5/2^+$, or $3/2^+$.

upper curves now indicate a slightly lower S factor in the region relevant to nova temperatures, whereas below 0.05 GK the S factor is more than an order of magnitude lower. The curves agree well with previous low-energy data (Refs. [4,12]) as well as the present work. It can be seen from Fig. 4 that the change in parity of the 8 keV state and resultant lack of interference with the 38- and 665 keV states has a significant effect on the uncertainty in the S factor in the region relevant to novae, reducing it from over a factor of 10 to around a factor of 2. However, this still results in up to a factor-of-10 uncertainty in the reaction rate [5]. An improved measurement at 250 keV could reduce this uncertainty by distinguishing between the upper and lower curves.

The preceding analysis is based on the assignments assumed in Ref. [5], and the resulting reaction rates are used by current nova models. However, the other assignments for the -121 keV resonance have not been excluded. Thus, for completeness, also shown in Fig. 4 are four curves corresponding to upper and lower limits on the S factor, assuming the -121 keV resonance to be either $5/2^+$ [23] or $3/2^+$ [9]. Now the range of possible S factors is significantly larger, particularly in the $3/2^+$ case due to interference with the 38- and 665 keV resonances. In both these cases, the experimental data favor the higher S-factor curves; however, confirmation of the spin of this state is required.

In conclusion, the lowest energy measurement to date of the astrophysically important ^{18}F$(p,\alpha)^{15}$O reaction was performed using a ^{18}F beam delivered by the ISAC radioactive beam facility at the TRIUMF laboratory, Canada. Measurements of the reaction cross section were made at four different energies and the calculated cross sections were used to constrain the R-matrix S-factor calculations at nova temperatures. It is clear that current knowledge of the level scheme of ^{19}Ne above the α threshold is incomplete and some of the accepted parameters may yet be shown to be inaccurate. Thus, there is a resultant uncertainty in R-matrix calculations based on incomplete data. Moreover, even if the state information on ^{19}Ne were complete, direct measurements of the cross section would still be needed to distinguish between the different interference possibilities. The present work is the first nonresonant measurement in the Gamow window for this reaction and thus the first to put significant constraints on the interference in the region relevant to novae. These data suggest that the cross section in the region of most importance to novae is either characterized by constructive interference between $3/2^+$ resonances at 38 and 665 keV and/or that there is a strong contribution from $1/2^+$ subthreshold states. This constraint on the cross section implies that stronger rates of destruction of ^{18}F in novae are preferred. Consequently, a lower abundance of ^{18}F, and thus a reduced detectability distance, is predicted. There remains, however, significant uncertainty in the nuclear physics, and further measurements, both direct and indirect, are needed.

We would like to thank the beam delivery and ISAC operations groups at TRIUMF. UK personnel were supported by the Science Technology Funding Council. Canadian authors were supported by the Natural Sciences and Engineering Research Councils of Canada. The authors would also like to thank P. Figuera, for the loan of the monolithic detector, and D. Bardayan, P. Descouvemont, N. de Séréville, J. José, and T. Histle for useful discussions.

[1] J. Jose and M. Hernanz, Eur. Phys. J. A **27**, 107 (2006).
[2] A. Coc *et al.*, Astron. Astrophys. **357**, 561 (2000).
[3] C. D. Nesaraja *et al.*, Phys. Rev. C **75**, 055809 (2007).
[4] D. Bardayan *et al.*, Phys. Rev. Lett **89**, 262501 (2002).
[5] C. Iliadis *et al.*, Nucl. Phys. A **841**, 31 (2010).
[6] M. Dufour and P. Descouvemont, Nucl. Phys. A **785**, 381 (2007).
[7] A. St. J. Murphy *et al.*, Phys. Rev. C **79**, 058801 (2009).
[8] J. C. Dalouzy *et al.*, Phys. Rev. Lett **102**, 162503 (2009).
[9] A. S. Adekola, Ph.D. thesis, Ohio University, 2009.
[10] D. W. Bardayan *et al.*, Phys. Rev. C **63**, 065802 (2001).
[11] J.-S. Graulich *et al.*, Phys. Rev. C **63**, 011302(R) (2000).
[12] N. de Séréville *et al.*, Phys. Rev. C **79**, 015801 (2009).
[13] F. Amorini *et al.*, Nucl. Instrum. Methods A **550**, 248 (2005).
[14] T. Davinson *et al.*, Nucl. Instrum. Methods A **454**, 350 (2000).
[15] Micron Semiconductor Limited, United Kingdom [www.micronsemiconductor.co.uk].
[16] H.-B. Mak *et al.*, Nucl. Phys. A **304**, 210 (1978).
[17] H. Lorenz-Wirzba *et al.*, Nucl. Phys. A **313**, 346 (1979).
[18] G. J. Feldman and R. D. Cousins, Phys. Rev. D **57**, 3873 (1998).
[19] K. Y. Chae *et al.*, Phys. Rev. C **74**, 012801(R) (2006).
[20] P. Descouvemont and D. Baye, Rep. Prog. Phys. **73** 036301 (2010).
[21] J. D. Garrett *et al.*, Phys. Rev. C **2**, 1243 (1970).
[22] S. Utku *et al.*, Phys. Rev. C **57**, 2731 (1998).
[23] A. Josephides, Ph.D. thesis, University of Edinburgh, 2009.